Relating the sequential dynamics of excitatory neural networks to synaptic cellular automata

V. I. Nekorkin, A. S. Dmitrichev, D. V. Kasatkin, and V. S. Afraimovich

Citation: Chaos **21**, 043124 (2011);
View online: https://doi.org/10.1063/1.3657384
View Table of Contents: http://aip.scitation.org/toc/cha/21/4
Published by the American Institute of Physics

Relating the sequential dynamics of excitatory neural networks to synaptic cellular automata

V. I. Nekorkin,[1] A. S. Dmitrichev,[1] D. V. Kasatkin,[1] and V. S. Afraimovich[2]
[1]*Institute of Applied Physics of RAS, 46 Ul'yanov Street, 603950, Nizhny Novgorod, Russia*
[2]*Instituto de Investigacion en Comunicacion Optica, Universidad Autonoma de San Luis Potosi, Karakorum 1470, Lomas 4a 78220, San Luis Potosi, S.L.P., Mexico*

(Received 24 January 2011; accepted 12 October 2011; published online 16 November 2011)

We have developed a new approach for the description of sequential dynamics of excitatory neural networks. Our approach is based on the dynamics of synapses possessing the short-term plasticity property. We suggest a model of such synapses in the form of a second-order system of nonlinear ODEs. In the framework of the model two types of responses are realized—the fast and the slow ones. Under some relations between their timescales a cellular automaton (CA) on the graph of connections is constructed. Such a CA has only a finite number of attractors and all of them are periodic orbits. The attractors of the CA determine the regimes of sequential dynamics of the original neural network, i.e., itineraries along the network and the times of successive firing of neurons in the form of bunches of spikes. We illustrate our approach on the example of a Morris-Lecar neural network. © *2011 American Institute of Physics*.
[doi:10.1063/1.3657384]

Real neural networks are extremely complex systems. They have a very complicated architecture of couplings, and individual neurons demonstrate nontrivial dynamics. Thus, the description of experimentally observed activity is often not a simple problem. Some neural processes (e.g., processes related to different cognitive tasks such as memory, attention, psychomotor coordination, etc.) are accompanied by transient short-time activity of individual neurons or small groups of neurons. In such a process, a sequence of activity phases of different neurons emerges successively in time, so, it is said to be a sequential dynamics. In the present article, we offer an approach of the reduction of continuous sequential dynamics of excitatory networks to a discrete one, in the form of a cellular automaton (CA) on the graph of connections. The reduction is based on the dynamics of synapses, but not neurons. We suggest a model of synapses in the form of a second-order system of nonlinear ODEs and show that there are two types of synaptic responses—the fast and the slow ones. The reduction of CA takes place if certain relations between the timescales of the responses hold. The regimes of sequential dynamics of the network are fully described by the attractors of the CA and consist of periodic (up to some accuracy) behavior of synapses and successive spike firing of neurons. We illustrate our approach on the example of a Morris-Lecar neural network.

I. INTRODUCTION

The neural systems comprised of neurons and glial cells[1] are known to exhibit a large variety of electrical activity. To study mechanisms of formation of different neural activities the approaches based on the dynamical systems paradigm are widely used.[2–7]

Neurophysiological experiments[8–10] have indicated that some neural processes (e.g., processes related to different cognitive tasks—memory, attention, psychomotor coordination, etc.) are accompanied by transient short-time activity of individual neurons or small groups of neurons. In such a process, a sequence of activity phases of different neurons emerges successively in time. It was shown within the dynamical systems framework[4,11–14] that this behavior is related to the existence of a collection of metastable invariant sets joined by heteroclinic trajectories in the phase space (the heteroclinic network), and thus can be thought of as a process of successive switchings among these metastable sets. There are some models in which the whole collection of metastable sets represented by either saddle equilibrium points[4,11,12] or saddle limit cycles[13] and the network of possible transitions between them can be rigorously established. However, sequential activity is not always directly related to the existence of a heteroclinic network. It was found in Ref. 15 that the excitable network of Morris-Lecar neurons can demonstrate a variety of sequential activity regimes which are formed by means of dynamical bifurcations. In such cases, in order to answer the main question of sequential dynamics—in which order neurons become activated—one needs to use a mathematical apparatus different from the heteroclinic channels technique.

Recently in Ref. 16 an approach for the study of neural networks has been proposed. It consists in reducing a given network to a discrete model. In this model[17] each neuron is represented by a finite number of states and there are rules

which determine how a neuron goes from one state to another. However, the approach has some limitations. It is based essentially on a specific character of the dynamics of neurons. Indeed, the neurons are assumed to be relaxational. In this case each neuron can be in one of three consecutive phases: active phase, when a neuron can excite other neurons, refractory phase, when a neuron is non-responsive to the action of other neurons, and rest phase, when a neuron can be excited (activated) by other neurons. The duration of the refractory phase is assumed to be a multiple of the duration of the active phase. Thus, the duration of the active phase is considered as a discretization time step. The interaction between neurons is taken into account in the following way. If a neuron receives an excitatory input, the excitation occurs instantaneously. On the other hand, if a neuron receives an inhibitory input, then it becomes excited due to the post-inhibitory rebound only when the inhibition ends. Moreover, the approach can be rigorously applied only to excitatory-inhibitory networks. In Ref. 18 the examples of application of this approach to specific biophysical models are presented.

Unlike,[16,18] in the present article we offer an approach which consist in reducing the continuous sequential dynamics of excitatory networks to a discrete one, in the form of a cellular automaton (CA) on the graph of connections, based on the dynamics of synapses with a short-term plasticity property. To account for the short-term plasticity property, we introduced a phenomenological model of a synapse in the form of a nonlinear system of ordinary differential equations (ODEs). Because of a special choice of nonlinear functions at the RHS of the system, two types of synaptic responses—fast and slow—are realized in the system, depending on external signals. This property lies at the base of the reduction of dynamics of the original network to a CA. The CA represents a network of synapses with a finite number of states which alternate with each other, according to some fixed rules. To determine the rules, we use both the theoretical knowledge of the dynamics of a synapse and the numerical study of its response to the incoming stimuli. But, we do not need to integrate numerically the whole system of ODEs representing the network which can be very large and complex. On the other hand, the CA describes adequately enough the main regimes of the sequential dynamics of synapses as well as of neurons of the whole network. This is the main advantage and attractiveness of our approach. Note that within a single activation-inactivation episode the dynamics of synapses is simple enough while the dynamics of neurons may be very complex. We demonstrate our approach on the example of Morris-Lecar neurons coupled by excitatory synapses with a short-term plasticity property.

The article is organized as follows. In Sec. II, we present the model of excitatory neural network with plastic synapses that we will use to illustrate our approach. In Sec. III, we study a model of synapses and describe the process of formation of neuron response. In Sec. IV, we construct a cellular automaton. In Sec. V, we briefly outline the scheme of application of the approach. In Sec. VI, we present a specific example of a CA for a network of four synaptically coupled neurons and discuss its relation to the dynamics of the original network. Section VII is devoted to the concluding remarks.

II. THE MODEL

For the sake of definiteness we illustrate our approach on the example of a neural network consisting of N Morris-Lecar neurons coupled by excitatory synapses with a short-term plasticity property. The dynamics of such a network is described by the following system of ODEs:

$$C\frac{dv_i}{dt} = -g_L(v_i - v_L) - g_{Ca}M_\infty(v_i)(v_i - v_{Ca}) - g_K n_i(v_i - v_K) + I_i^{ext} - g_{syn}s_i(v_i - v_{rev}), \quad (1)$$

$$\frac{dn_i}{dt} = \frac{n_\infty(v_i) - n_i}{\tau_n(v_i)}, \quad (2)$$

$$\frac{dr_i}{dt} = f_1(r_i) - s_i - k_1, \quad (3)$$

$$\frac{ds_i}{dt} = \varepsilon(f_{2i} - s_i - k_2). \quad (4)$$

Each neuron (Eqs. (1) and (2)) of the network is described by the Morris-Lecar model.[19] The variables v_i, n_i characterize the membrane potential and the activation of the potassium ion channels of the i-th neuron ($i = 1, ..., N$), C is the membrane capacitance. The terms at the RHS of Eq. (1) describe the currents flowing through the cell membrane of a neuron. The first three terms determine the leakage, the calcium and the potassium ionic currents, respectively, g_L, g_{Ca}, g_K are the maximal conductances, v_L, v_{Ca}, v_K are the equilibrium (reverse) potentials for the corresponding ion channels, and $M_\infty(v)$, $n_\infty(v)$, $\tau_n(v)$ are the stationary states of the activation levels and the characteristic relaxation time, respectively, depending on the membrane potential by the sigmoid law:

$$M_\infty(v) = 0.5\left[1 + \tanh\left(\frac{v - v^{(1)}}{v^{(2)}}\right)\right],$$
$$n_\infty(v) = 0.5\left[1 + \tanh\left(\frac{v - v^{(3)}}{v^{(4)}}\right)\right],$$
$$\tau_n(v) = \left[\phi\cosh\left(\frac{v - v^{(3)}}{2v^{(4)}}\right)\right]^{-1},$$

where $v^{(1)} = -0.01$, $v^{(2)} = 0.15$, $v^{(3)} = 0$, $v^{(4)} = 0.3$, $\phi = 1$. The term I_i^{ext} is an external current. The last term at the RHS of Eq. (1) determines the synaptic current emerging as a result of action of other neurons on the i-th neuron by chemical synapse, where g_{syn} is the maximum synaptic conductance, v_{rev} is synaptic reversal potential and variable s_i corresponds to the fraction of open synaptic channels. To describe a short-term plasticity property, we introduced a phenomenological model of synapse in the form of a system of Eqs. (3) and (4). In Eq. (3), $f_1(r)$ is a piecewise linear (PWL) continuous function which resembles the shape of a fifth-degree polynomial:

$$f_1(r) = \begin{cases} -\gamma_1 r - A(1+\sigma_1), & r \le -x_0 \\ \gamma_2 r, & -x_0 < r \le x_0 \\ -\gamma_3 r + A(1+\sigma_3), & x_0 < r \le x_1 \\ \gamma_4 r - A(1+\sigma_4), & x_1 < r \le x_2 \\ -\gamma_5 r + A(1+\sigma_5), & r > x_2 \end{cases} \quad (5)$$

where

$$\sigma_1 = \frac{\gamma_1}{\gamma_2}, \quad \sigma_3 = \frac{\gamma_3}{\gamma_2}, \quad \sigma_4 = \frac{\gamma_4}{\gamma_2} + 2\frac{\gamma_4}{\gamma_3},$$
$$\sigma_5 = \frac{\gamma_5}{\gamma_2} + 2\gamma_5\left(\frac{1}{\gamma_4} + \frac{1}{\gamma_3}\right),$$
$$x_0 = \frac{A}{\gamma_2}, \quad x_1 = A\left(\frac{1}{\gamma_2} + \frac{2}{\gamma_3}\right), \quad x_2 = A\left(\frac{1}{\gamma_2} + \frac{2}{\gamma_3} + \frac{2}{\gamma_4}\right)$$

with $A = 2/3$, $\gamma_1 = 0.1$, $\gamma_2 = 1.136$, $\gamma_3 = 5$, $\gamma_4 = 41.113$, $\gamma_5 = 20$.

In Eq. (4), f_{2i} is a monotonically increasing continuous PWL function:

$$f_{2i} = \begin{cases} [\alpha + \mu\zeta_i\chi_i]r_i, & r_i < 0 \\ \beta r_i, & r_i \ge 0 \end{cases} \quad (6)$$

where $\chi_i = \sum_{\substack{j=1, \\ j\neq i}}^{N} H(v_j - \theta_{ji})$, $\zeta_i = H(\theta_{ref} - s_i)$ and $H(x) = 1/(1+\exp(-x/1000))$ is a smooth approximation of the Heaviside step function. The term χ_i describes an action of presynaptic neurons on the synapse of ith neuron. Parameters θ_{ji} characterize the initial instants of activation of synaptic processes caused by input signals, i.e., they determine the synaptic thresholds. The term ζ_i accounts for the refractory property of a synapse. It is equal to 1 only while the synapse is not activated ($s_i < \theta_{ref}$). The choice of functions (5) and (6) will be motivated in Sec. III A. Note only that the PWL form of functions (5) and (6) is chosen for the simplicity of analysis. As our numerical results show, these functions can be replaced by their smooth analogs without any major influences on the dynamics of a synaptic model.

III. DYNAMICS OF A SYNAPSE AND NEURON RESPONSE ON A SYNAPTIC ACTION

Here, we study the dynamics of the proposed phenomenological model of a synapse, describe the process of formation of neuron response and formulate the basic properties of synapses and neurons which allow us to reduce the continuous dynamics of neural networks to a discrete one.

A. Conventional models of synapses and a biophysical foundation of our model

Let us first outline the general biophysical mechanisms underlying the synaptic transmission. In a chemical synapse (CS) the membranes of interacting (pre- and postsynaptic) neurons are separated by a sufficiently wide synaptic cleft.[1] In such a synapse the presynaptic action potential depolarizes the membrane of presynaptic cell. It leads to the opening of the voltage-gated calcium channels, causing an influx of calcium ions and a modulation of calcium concentration through calcium buffering. A certain calcium concentration triggers the exocytosis of readily releasable vesicles (the docking and priming of synaptic vesicles, the fusion between the vesicles and the presynaptic cell membrane, the opening of the vesicles) with the subsequent release of the neurotransmitter into the synaptic cleft. Vesicles are then retrieved by endocytosis, recycled and refilled with the neurotransmitter. A part of the released neurotransmitter molecules diffuse within the cleft and then bind to receptors on the postsynaptic cell membrane. The binding directly or indirectly leads to the opening of the ion channels. The opening causes an ion flux across the postsynaptic cell membrane, the synaptic current, changing its local transmembrane potential.

There exist several widely used models of CS which are distinguished, in fact, by the description of evolution of the synaptic conductance. According to the conductance-based formalism, the synaptic current may be defined as follows:

$$I_{syn} = g(t)(V_{post} - V_{rev}),$$

where V_{post} is the membrane potential of postsynaptic cell, V_{rev} is the synaptic reversal potential, and $g(t)$ reflects the time course of the synaptic conductance change.

The popular way to describe the synaptic conductance change is the alpha function[20]:

$$g(t) = g_{syn}\frac{t - t_k}{\tau}\exp[-(t - t_k)/\tau], \quad (7)$$

where g_{syn} is the maximum conductance, τ specifies the characteristic timescale of the response, and t_k is the time when the presynaptic cell triggers the spike.

Another widely used way to model the synaptic conductance change is based on a simple two-state (open/close) kinetic scheme[21] of the neurotransmitter-receptor interaction. It is also assumed that the spike incoming onto the presynaptic cell induces a brief and a uniform increase of a neurotransmitter concentration in the synaptic cleft. In such a case the conductance $g(t) = g_{syn}s(t)$, where $s(t)$ denotes the fraction of open channels and is defined by

$$\frac{ds}{dt} = \alpha[T](1 - s) - \beta s. \quad (8)$$

Here α and β are the rates of opening and closing of ion channels, respectively, $[T]$ is the neurotransmitter concentration depending on the presynaptic membrane potential V_{pre} by the following law:

$$[T](V_{pre}) = \frac{T_{max}}{1 + \exp[-(V_{pre} - V_p)/K_p]},$$

where T_{max} is the maximal concentration of neurotransmitter in the synaptic cleft, K_p gives the steepness and V_p sets the value at which the function is half-activated.

The models (7) and (8) are computationally very efficient, but do not take into account some aspects of dynamical regulation of the synaptic transmission, in particular, the so-called synaptic plasticity, i.e., the ability of synapses to change their efficacy depending on the activity of pre- and postsynaptic cells.

Here, we focus only on transient (short-term) changes[22] which persist for milliseconds to seconds. Recently a number of phenomenological[23–26] and biophysically tractable[27–34] models incorporating different pre- and/or postsynaptic processes have been proposed to describe short-term plasticity. Usually the models take into account the following presynaptic processes: changing of the probability of the vesicle fusion due to accumulation of "residual" calcium (calcium buffering), recovery and depletion of the readily releasable pool of vesicles. The competition of these processes determines the neurotransmitter release rate. In particular, it is shown in Ref. 28 that the vesicles release probability and the amount of readily releasable vesicles have the opposing trends with the varying presynaptic stimulation frequency. It leads to a resonance dependence of the rate of neurotransmitter release on the frequency of stimulation. A high resonance frequency indicates the facilitation of neurotransmitter release whereas a low resonance frequency suggests the depression of neurotransmitter release. Note that the rate of the neurotransmitter release affects the rate of the opening of postsynaptic ion channels (see, e.g. Eq. (8)). In our model (see Eqs. (3) and (4)) aforementioned facilitation is included by means of existence of two responses (the slow and the fast ones) depending on the presynaptic stimulus rate. The responses differ in characteristic rise rate of s-variable (rate of the postsynaptic ion channels opening). The smaller rise rate is for the low stimulus rate and the higher one is for the high stimulus rate. On the other hand, receptor desensitization, i.e., transition of receptors in a state non-responsive to the neurotransmitters, are usually taken into account among postsynaptic processes. The desensitization influences the formation of synaptic responses during repeated activation of the receptors. In particular, such a process can affect the synaptic temporal behavior in several ways,[29,34] including the prolongation of the decay time and the shortening of the rise time. Also it has been shown that the desensitization plays a crucial role only at high presynaptic cell stimulation frequencies. In our model the receptor desensitization is included as bounding of rise time of s-variable (bounding of channels opening time) for high-rate presynaptic stimulation (in the case of fast response). Thus in our model presynaptic facilitation and postsynaptic desensitization are taken into account by means of existence of two types of synaptic responses which have different rise rates of s-variable and almost equal amplitudes.

Note that the known models of CS with short-term plasticity properties which scrupulously describe the pre- and postsynaptic mechanisms are high-order dynamical systems. Such a detailing in the modeling of processes in CS for the study of spatio-temporal activity of large networks seems to be unnecessary. Therefore, we have proposed a simple enough phenomenological model of CS in the form of a second-order system of nonlinear ODEs. In this model, we reflect the above listed features by means of using the relaxational behavior of Eqs. (3) and (4) and a special design of nonlinear functions (5) and (6). In this case any trajectory of the system consists of slow (in a vicinity of stable manifold of slow motions corresponding to falling parts of the curve $s=f_1(r)-k_1$) and fast ($s\approx const$) pieces (see below, for details). There are three branches of stable manifold of slow motions. One of them lies in the half plane $r<0$. The evolution of the system along this branch corresponds to inactivation phase of synaptic coupling. Two other branches lie in the half plane $r>0$. The evolution of the system along each of these branches corresponds to a certain scenario of activation (response) of synaptic coupling. The choice of one of the two branches depends on the form of presynaptic stimulation (waveform of $\chi_i(t)$).

B. The study of the system of Eqs. (3) and (4) for $\mu=0$

Let us now consider the dynamics of the system of Eqs. (3) and (4) for $\mu=0$. In this case one can rewrite the system in the following form:

$$\begin{cases} \dot r = f_1(r) - s - k_1, \\ \dot s = \varepsilon(f_2(r) - s - k_2), \end{cases} \tag{9}$$

where $f_2(r)=\alpha r$ for $r<0$ while $f_2(r)=\beta r$ for $r\geq 0$.

Let $\varepsilon \ll 1$: Then the variable s is changing more slowly in time than the variable r, i.e. in the system (9) there are two different time and velocity scales. Fast motions are determined mainly by the frozen system (9) for $\varepsilon=0$, i.e., by the system:

$$\begin{cases} s = const, \\ \dot r = f_1(r) - s - k_1. \end{cases} \tag{10}$$

Slow motions are described by the equation for the variable s depending nevertheless on the state of the fast variable at the quasi-equilibrium state, i.e., by the system

$$\begin{cases} s = f_1(r) - k_1, \\ \dot s = \varepsilon(f_2(r) - s - k_2). \end{cases} \tag{11}$$

Because of the interaction of the fast and slow variables, each trajectory of the system (9), in fact, will consist of alternating slow (in a vicinity of the curve $s=f_1(r)$) and fast ($s\approx const$) pieces. Such motions are said to be relaxation oscillations.

Let the parameters of the system (9) meet the requirements:

$$\beta > \gamma_2\left(1+\frac{k_2-k_1}{A}\right), \quad k_1<k_2, \quad k_1>k_2-A, \quad \varepsilon<\gamma_2. \tag{12}$$

and α be a control parameter. It is easy to see that under the condition $\alpha<\gamma_2(1-\frac{k_2-k_1}{A})$ the system (9) has the following three equilibrium states: $O_0(r_0,\ s_0)$, $O_1(r_1,\ s_1)$, $O_2(r_2,\ s_2)$, where

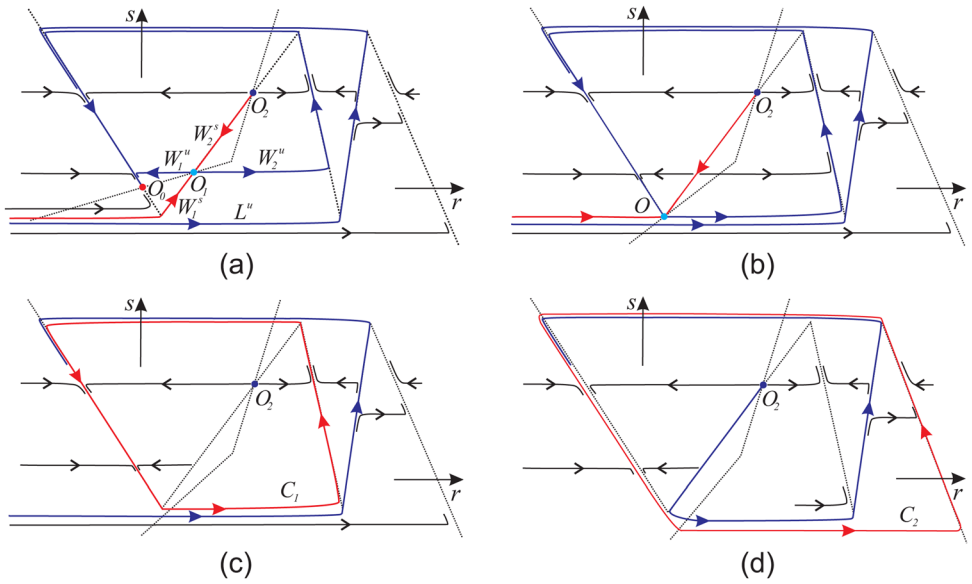

FIG. 1. (Color online) The phase portraits of the system (9) which correspond respectively to (a) $\alpha < \gamma_2(1-\frac{k_2-k_1}{A})$; (b) $\alpha = \gamma_2(1-\frac{k_2-k_1}{A})$; (c) $\gamma_2(1-\frac{k_2-k_1}{A}) < \alpha < \alpha^*$; and (d) $\alpha > \alpha^*$. The other parameters satisfy the conditions (12). The dashed curves on figures are nullclines.

$$r_0 = -\frac{A\left(1+\frac{\gamma_1}{\gamma_2}\right)-k_2+k_1}{\alpha+\gamma_1},\quad s_0 = -\frac{\alpha A\left(1+\frac{\gamma_1}{\gamma_2}\right)+\gamma_1\kappa_2+\alpha\kappa_1}{\alpha+\gamma_1},$$
$$r_1 = -\frac{k_2-k_1}{\gamma_2-\alpha},\quad s_1 = \frac{k_1\alpha-k_2\gamma_2}{\gamma_2-\alpha},$$
$$r_2 = \frac{k_2-k_1}{\beta-\gamma_2},\quad s_2 = -\frac{k_2\gamma_2-k_1\beta}{\beta-\gamma_2}. \tag{13}$$

The equilibrium state O_0 is asymptotically stable (the focus or the node), the state O_2 is the repeller, and O_1 is the saddle point. The corresponding phase portrait of the system (9) is shown on Fig. 1(a). We denote by W_1^s, W_2^s and W_1^u, W_2^u the incoming (correspondingly outcoming) separatrices of the saddle belonging to its stable (correspondingly unstable) manifold. In this case all trajectories except O_1, O_2 and stable separatrices of O_1 go asymptotically to the equilibrium state O_0. Here, L^u is the trajectory containing a piece of the unstable manifold of the system (9) with the slope close to γ_4. We will show that such a trajectory plays a crucial role in the formation of short-term plasticity properties in our phenomenological model of a synapse. For $\alpha = \gamma_2(1-\frac{k_2-k_1}{A})$ the equilibrium states O_0 and O_1 merge forming the equilibrium state $O(r=-\frac{A}{\gamma_2}, s=-A-k_1)$ of the saddle-node type. It has a stable node region and an unstable separatrix. The phase portrait of the system (9) in this case is shown on Fig. 1(b). Here the separatrices of O form a homoclinic trajectory. Further increasing of the parameter α leads to the disappearance of O and of the homoclinic trajectory as well. In the vicinity of homoclinic trajectory a stable limit cycle C_1 appears, see Fig. 1(c). The limit cycle C_1 exists up to some value $\alpha = \alpha^*$. The dependence of α^* on the parameters of the system has complex enough form so we do not illustrate it here. For this value of α, the fast pieces of the cycle C_1 merge with the fast pieces of the trajectory L^u and the cycle C_1 vanishes. The disappearance of C_1 is accompanied by the creation of a new stable limit cycle C_2. It is formed on account of slow motions in a neighborhood of an invariant line with the slope close to $-\gamma_5$ (Fig. 1(d)). The limit cycle C_2 exists for all values of the parameters $\alpha > \alpha^*$.

C. Activation of synaptic coupling

Here we consider the process of the activation of i-th synaptic coupling. For definiteness we fix the parameters in Eqs. (3) and (4):

$$\alpha = 0.2,\quad \beta = 2,\quad k_1 = -0.616,\quad k_2 = -0.216,$$
$$\varepsilon = 0.005,\quad \mu = 2.3,\quad \theta_{ref} = 0.01. \tag{14}$$

Let us start from the case when $v_j < \theta_{ji}$ holds for all presynaptic neurons, i.e., terms $H(v_j - \theta_{ji}) = 0$ for all j. Then $\chi_i = 0$ and the Eqs. (3) and (4) coincide with the equations of the system (9). Under the chosen values of parameters the system (9) has the phase portrait shown on Fig. 1(a). Here, the regime corresponding to the stable equilibrium point O_0 is globally stable. Note that the parameters k_1 and k_2 are chosen in such a way that the s-coordinate of this equilibrium equals 0. Hence $\zeta_i = 1$ and the i-th synapse can be activated.

Let us assume now that at some instant of time the potentials of one or several neurons v_j exceed the threshold values θ_{ji}. Then χ_i takes quickly some positive value which is approximately equal to the number of neurones whose membrane potentials satisfy the condition $v_j > \theta_{ji}$ at a given instant of time. It follows that during the time interval for which $v_j > \theta_{ji}$ the Eqs. (3) and (4) again will coincide with the ones for the system (9). However, their dynamics will be determined now by a new effective value of the parameter α: $\alpha_{new} = \alpha + \mu\chi_i$, i.e.,

$$\begin{cases} \dot r = f_1(r) - s - k_1, \\ \dot s = \varepsilon(\widetilde{f_2}(r) - s - k_2), \end{cases} \tag{15}$$

where

$$\widetilde{f_2}(r) = \begin{cases} [\alpha+\mu\chi_i]r, & r < 0, \\ \beta r, & r \ge 0. \end{cases}$$

Depending on the value of χ_i the system (15) has a phase portrait shown either on Fig. 1(c) realizing for $\chi_i < \chi_i^* = \frac{\alpha^*-\alpha}{\mu}$ (for Eq. (14) $\alpha^* = 0.6128$) or on Fig. 1(c) realizing for

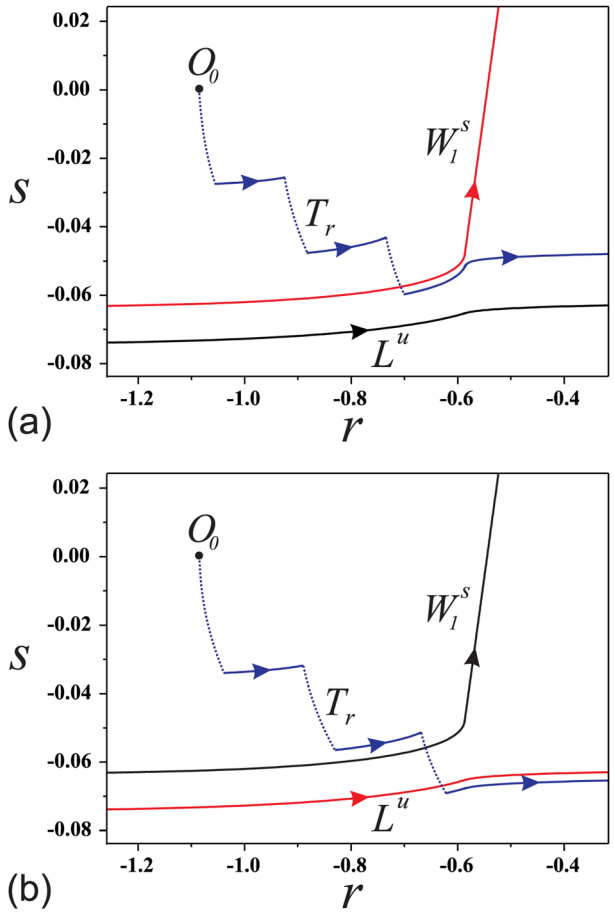

FIG. 2. (Color online) The fragments of trajectories formed in the coupling subsystem of Eqs. (3) and (4) as a result of the processes of its activation and inactivation for (a) weak and (b) strong stimulations. In both cases the stimulation $\chi_i(t)$ represents a sequence of three square pulses with the same amplitude and duration. The amplitude of pulses equals 1; the durations are (a) 3 and (b) 6. The parameters are given by Eq. (14).

$\chi_i > \chi_i^*$. It is not difficult to see that in both cases the only attractor of the system is the limit cycle (C_1 or C_2). Let us remark that the initial conditions for the system (3) and (4) (and so for the system (15)) are determined by the dynamics of the former system (9) and correspond to the coordinates of its equilibrium state O_0. Thus the trajectory of the system (15) starting at O_0 goes to a vicinity of the stable limit cycle being governed by the system (15). Once all variables v_j become less than θ_{ji}, the dynamics of the system will again be described by Eqs. (9) and the trajectory comes back to a vicinity of O_0.

Thus the dynamics of the synapse is governed by the alternating action of two systems: Eqs. (9) and (15). If the exceeding of potentials v_j over values of θ_{ji} is multiple then a glued trajectory T_r (Figs. 2(a) and 2(b)) appears on the (r_i, s_i)-plane. It consists of alternating pieces of trajectories of the system (9) (dotted lines) and of the system (15) (continuous lines). The process of formation of the glued trajectory T_r is ended when the inequalities $v_i(t) < \theta_{ji}$ hold for all j. The further dynamics is fully determined by the system (9). Two possibilities can occur. If the representing point of the trajectory lies on the right side of the separatrix W_1^s (Fig. 1(a)) or on the right side of the unstable manifold L^u (Fig. 1(a)), then the trajectory T_r comes to a vicinity of the equilibrium point O_0 according to the dynamics of the system (9). It is accompanied by a "powerful" change of the variable r, i.e., an activation of the synaptic coupling takes place. Here, the evolution of the variable s has a form typical for the synaptic current (see Fig. 3). Moreover, during the activation period $s_i > \theta_{ref}$, then $\zeta_i = 0$. Therefore the synapse becomes nonsensitive to the presynaptic stimulation. It reflects refractory property of synapse. On the other hand, if the representing point on the (r_i, s_i)-plane lies on the left side of W_1^s or L^u, the trajectory T_r again goes to O_0 but the relevant impulse response does not appear. In this case there is no activation of the synaptic coupling.

The separatrix W_1^s and the unstable manifold L^u determine two thresholds of activation of the synaptic coupling. In order to go through the first threshold (Fig. 2(a)) it is sufficient to have a comparatively weak pre-synaptic effect. On the other hand, for the overcoming of the second threshold, the pre-synaptic action should be sufficiently strong (Fig. 2(b)). Moreover, the overcoming of different thresholds leads to the different efficiency of the activation of synaptic coupling, i.e., different characteristic times of the growth of the synaptic current (intervals T_1 and T_2 during which $s(t)$ increases from 0 to its maximal value, see Fig. 3). In the first case (weak pre-synaptic action) the growth of the synaptic current occurs slowly. Here, the trajectory T_r goes in the vicinity of stable branch of manifold of slow motions characterized by the slope close to $-\gamma_3$. In the other case, the strong pre-synaptic effect causes comparatively fast growth

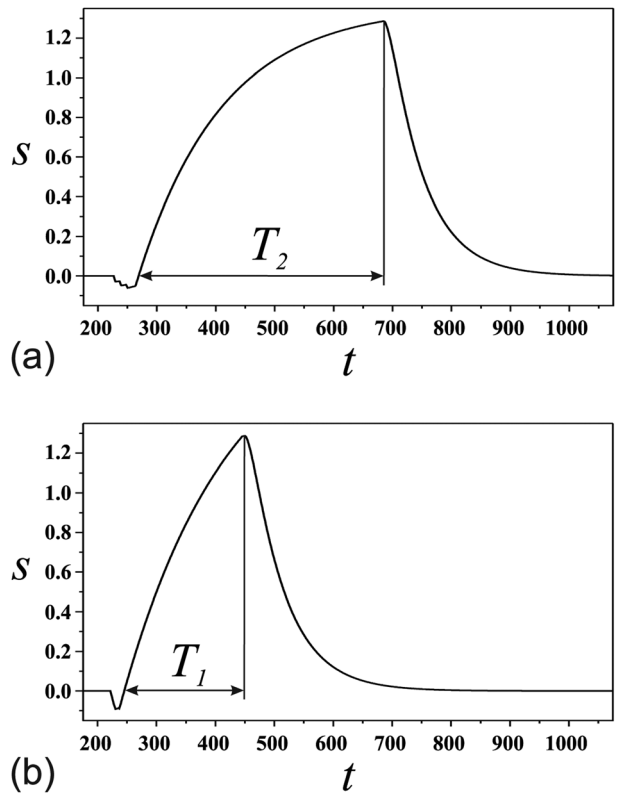

FIG. 3. Waveforms of the synaptic variable in the case of (a) slow and (b) fast synaptic responses. They correspond to trajectories T_r depicted on Figs. 2(a) and 2(b), respectively.

of the synaptic current. Here, the trajectory T_r goes in the vicinity of stable branch of manifold of slow motions characterized by the slope close to $-\gamma_5$. For the chosen values of parameters the condition $T_2 \simeq 2T_1$ takes place.

Note that the existence of slow and fast responses in our model reflects one of the important features of chemical synapses called synaptic plasticity which is characterized, generally, by the nontrivial dependence of the synaptic response on the form of presynaptic action. The system (3) and (4) models also another feature of synapses called synaptic delay. Here, it is determined by the time that is necessary for the representative point to appear on the right side of one of the described thresholds.

Finally let us summarize the basic properties of the synapse which we will use next:

(*E1*) There are two types of responses (slow and fast) of the synapse to different stimuli.

(*E2*) The characteristic times of the growth of the slow and fast synaptic responses satisfy the "resonance" condition $T_2 = 2T_1$.

(*E3*) When a synapse is active it is non-sensitive to the presynaptic stimulation.

Let us emphasize that exact resonance condition $T_2 = 2T_1$ is never realized since the activation of the i-th neuron occurs when the value of function $s_i(t)$ belongs to a neighbourhood of its maximum. The size of the neighbourhood depends on many factors which are impossible to control. Nevertheless, even the approximate validity $(T_2 \simeq 2T_1)$ of this condition is sufficient to describe the sequential dynamics as we show below. This signifies the robustness of our approach.

D. Response of a neuron to synaptic action

Let us discuss now the basic properties of a neuron response to an excitatory synaptic action generated by the system of Eqs. (3) and (4). We consider the process of formation of the response on the example of Morris-Lecar neuron (the system of Eqs. (1) and (2)). Here, we use the following values of parameters:

$$C = 1.4, \quad g_L = 0.1, \quad g_{Ca} = 1.1, \quad g_K = 2, v_L = -0.5,$$
$$v_{Ca} = 1, \quad v_K = -0.7, \quad I_i^{ext} = 0.13, \quad g_{syn} = 0.0409,$$
$$v_{rev} = 0.5. \tag{16}$$

The parameters are chosen so that the neuron is at rest in the absence of synaptic current. Moreover the choice of the v_{rev}-value corresponds to the case of excitatory synaptic coupling.

Under the action of the synaptic current $I_{syn}(t)$ the system (1) and (2) describing the i-th neuron may be treated as non-autonomous and, therefore, it has three-dimensional generalized phase space. The system (3) and (4) have a small parameter ε and therefore, the evolution of the s_i-variable is slow with respect to the evolution of v_i and n_i. Hence, in the first approximation $s_i(t)$ may be considered as a parameter that is changing slowly. On Fig. 4(a) a fragment of the bifurcation diagram of the system (1) and (2) are presented. For

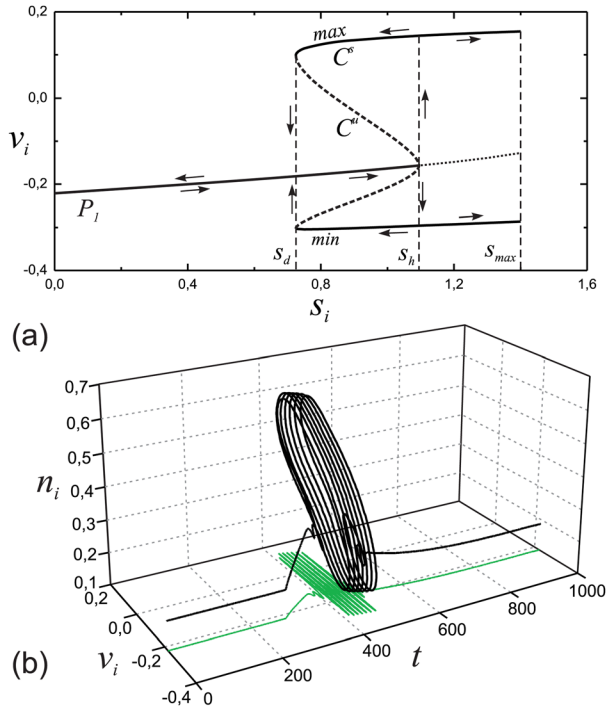

FIG. 4. (Color online) (a) Bifurcation diagram and (b) a trajectory in the non-autonomous phase space. The parameters are given by Eq. (16).

$s_i < s_d \simeq 0.724$ the only equilibrium state P_1 exists. For $s_i = s_d$ the saddle-node bifurcation of a limit cycle holds, and two limit cycles—stable C^s and unstable C^u-appear on the phase plane. Further increasing of s_i leads to the shrinking of C^u to the equilibrium state P_1, and for $s_i = s_h \simeq 1.092$ the equilibrium state P_1 changes its stability due to the subcritical Andronov-Hopf bifurcation. In the generalized phase space the stable equilibrium states $P_1(s_i)$ form a stable one dimensional integral manifold $M^s_{st}(0)$ and the stable limit cycles C^s form a stable two-dimensional integral manifold $M^s_c(0)$. According to the theorem of persistence of integral manifolds (see, e.g., Refs. 35 and 36), there are integral manifolds $M^s_{st}(\varepsilon)$ and $M^s_c(\varepsilon)$ close to $M^s_{st}(0)$ and $M^s_c(0)$ correspondingly. Since initially the i-th neuron is at the phase of rest, the representative point in the generalized phase space is situated on the manifold $M^s_{st}(\varepsilon)$. Under a synaptic action the representative point starts moving along $M^s_{st}(\varepsilon)$ until it reaches the boundary of $M^s_{st}(\varepsilon)$. Due to a special choice of the parameter g_{syn} in the expression for the synaptic current, this piece of the itinerary of the representative point corresponds to the interval of the increasing of the variable $s_i(t)$ until it reaches its maximal value. After that the representative point passes rapidly into a vicinity of $M^s_c(\varepsilon)$ forming an oscillatory motion in the opposite direction (Fig. 4(a)). This piece of its itinerary corresponds to the decreasing part of the graph of $s_i(t)$ from the maximal value (Fig. 3). The oscillating process is over when the representative point reaches the boundary of the manifold $M^s_c(\varepsilon)$. As a result, a "transitive oscillating set" (see Fig. 4(b)) is forming in the generalized phase space. It corresponds to the generation of a collection of spikes in the i-the neuron. Because of our choice of parameters, the temporal intervals of the generation are relatively short with respect to the time-scales of the synaptic response. Thus, in fact, the neuron can

be in one of two states having different temporary scales: one of them corresponds to the slow monotonous change of the membrane potential v_i and the other—to the fast generation of spikes (Fig. 4). In addition, these processes differ for the fast and slow synapses only by the duration of the slow phase of the change of v_i, and the spike oscillations in both cases are practically the same.

Finally let us note main features of the dynamics of neuron subjected to an excitatory synaptic action:

(*E4*) The time course of synaptic conductance (evolution of s_i) completely determines the dynamics of a neuron.

(*E5*) The neuron is at rest in the absence of synaptic current (the conductance $s_i = 0$).

(*E6*) The generation of spikes starts (due to, e.g., subcritical Andronov-Hopf bifurcation) when the synaptic conductance overcomes some threshold value which is close to maximum of s_i.

(*E7*) The temporal intervals of generation of spikes are relatively short with respect to the characteristic timescales of evolution of s_i.

Though we considered here the Morris-Lecar neuron, similar properties are observed in other models of neurons.

IV. CONSTRUCTION OF CELLULAR AUTOMATA ON THE GRAPH

Let us consider an excitatory neural network consisting of N neurons. We assume that neurons and synapses of the network possess the properties described above, i.e., satisfy the requirements (*E1*)-(*E7*). Because of that it is possible to give a description of continuous dynamics of such a network in terms of a discrete one using the ideas of symbolic dynamics. We shall define a simple dynamical system in the form of a finite state automaton or, as we will call it, a cellular automaton on the graph (see Appendix).

A. Graph of connections

Let us define directed graph $G = \langle Q_G, K_G \rangle$. It has N vertices $Q_G = \{Q_1, Q_2, ..., Q_N\}$ which signify the synapses of the network. The set $K_G = \{K_1, K_2, ..., K_N\}$ reflects the architecture of the connections in the network. Each K_i is a collection of indices such that $j \in K_i$ if and only if there is a connection from the j-th synapse of the network to the i-th synapse through the j-th neuron. This possibility follows from the property (*E4*).

B. Discrete states of a synapse

We will define discrete states of a synapse according to the behavior of the s-variable describing its dynamics. Here we use the properties (*E1*) and (*E2*). We say that the i-th synapse is in the state $\psi_i(s_i)$ that is equal to:

- P_{11} if $s_i(t)$ undergoes the fast response and $s_i'(t) > 0$ (see Fig. 3(b));
- P_{21} if $s_i(t)$ undergoes the response of the slow type, $s_i'(t) > 0$ and $t_{in} \le t \le T_1 + t_{in}$, where $s_i(t_{in}) = 0$, $s_i'(t_{in}) > 0$, i.e., $s_i(t)$ starts growing at the instant of time t_{in} (see Fig. 3(a));
- P_{22} if $s_i(t)$ again undergoes the response of the slow type and $s_i'(t) > 0$, but $T_1 + t_{in} \le t \le 2T_1 + t_{in}$;
- P_0 if it is not in one of the previous states, i.e., either it is in the equilibrium state $s_i(t) = 0$ or $s_i'(t) < 0$ in both the slow and fast cases (see Fig. 3).

Thus, we have replaced the continuous description of the behavior of the i-th synapse in terms of $s_i(t)$ by a discrete description in terms of $\psi_i = \psi_i(s_i)$. The set of values of ψ_i, $i = 1,...,N$, is the collection of the symbols $\mathcal{P} = \{P_0, P_{11}, P_{21}, P_{22}\}$. For the sake of convenience we identify P_0 with 0, P_{11} with 1, P_{21} with 2, and P_{22} with 3, so $\mathcal{P} = \{0, 1, 2, 3\}$. We will use both notations below.

C. The rules of CA

Now we define the rules of evolution in time of ψ_i, i.e., the rules of a CA. They can be formulated on the basis of properties (*E3*), (*E5*)-(*E7*).

(i) If i-th synapse at the instant of time t is in the state P_0 ($\psi_i(s_i(t)) = P_0$), and there is $j \in K_i$ such that $\psi_j(s_j(t)) = P_{11}$ or $\psi_j(s_j(t)) = P_{22}$ then it will be excited at the instant $t + T_1$, i.e., $\psi_i(s_i(t + T_1)) = P_{11}$ or $\psi_i(s_i(t + T_1)) = P_{21}$ depending on the values of threshold constants θ_{ji}.

(ii) If i-th synapse at the instant of time t is in the state P_{21}, i.e., $\psi_i(s_i(t)) = P_{21}$, then $\psi_i(s_i(t + T_1)) = P_{22}$, independently of other synapses. Moreover, the P_{21}-synapse cannot excite another synapse.

(iii) If $\psi_i(s_i(t)) = P_{11}$ or $\psi_i(s_i(t)) = P_{22}$, then $\psi_i(s_i(t + T_1)) = P_0$, independently of the states of other synapses.

(iv) Because of the existence of the refractory period, the synapses in the states P_{11}, P_{21}, P_{22} do not feel the action of other synapses.

These statements imply that for the fixed i the state $\psi_i(s_i(t + T_1))$ at the instant $t + T_1$ is uniquely determined by:

- the state $\psi_i(s_i(t))$ at the previous instant of time t;
- the states of the j-th synapse, $j \in K_i$, at the instant of time t;
- the values of the threshold constants θ_{ji}, $j \in K_i$.

Hence,

$$\psi_i(s_i(t + T_1)) = F_i(\psi_i(s_i(t)),\ \{\psi_j(s_j(t))\},\ \{\theta_{ji}\}, j \in K_i), \tag{17}$$

where F_i is a function determined by the statements (*i*)-(*iv*). The relation (17) is a synaptic CA determined on the graph of connections G. In Table I we summarize the rules of the CA. In what follows we identify $\psi_i(s_i(t))$ with the symbol ψ_i and $\psi_i(s_i(t + T_1))$ with the symbol $\overline{\psi_i}$.

Let us clarify how to use the table. If, for example, $\psi_i = P_{11}$ and $\psi_j = P_0$, $j \in K_i$, then $\overline{\psi_i} = P_0$; but if $\psi_i = P_{21}$, $\psi_j = P_{21}$, $j \in K_i$, then $\overline{\psi_i} = P_{22}$.

Finally if we fix the values of thresholds θ_{ji} the rules of the CA take the following form:

$$\overline{\psi_i} = F_i(\psi_i, \{\psi_j\}, j \in K_i), \tag{18}$$

where $\overline{\psi_i}, \psi_i \in \mathcal{P}$.

TABLE I. Rules of the synaptic CA.

ψ_i	P_0	P_{11}	P_{21}	P_{22}
$\psi_j, j \in K_i$ $\forall j \in K_i, \psi_j = P_0$ or $\psi_j = P_{21}$	P_0	P_0	P_{22}	P_0
$\exists j \in K_i$, such that $\psi_j = P_{11}$ or $\psi_j = P_{22}$	P_{11} or P_{21} depending on the values of threshold constants θ_{ji}	P_0	P_{22}	P_0

V. SCHEME OF THE APPLICATION OF THE APPROACH

Consider an arbitrary excitatory network consisting of N neurons. The following scheme of the application of our approach follows immediately from the aforementioned results.

1. Single out the elementary clusters of the neural network and construct the graph of connections $G = <Q_G, K_G>$ (see Sec. IV). The cluster B_i ($i = 1,...,N$) is defined as part of the network including the i-th synapse and j-th synapses coupled with the i–th one through j-th neurons.
2. Determine the responses of each cluster. In other words for each $i = 1,...,N$, find the responses of the i-th synapse caused by the different (fast and slow) actions of the j-th synapse through the j-th neuron, $j \in K_i$. It is implied that a collective action of groups of several j-th synapses also has to be studied (if K_i consists of more than one element).
3. Using the responses define the rules of the CA, according to Table I.
4. Study dynamics of CA, find its attractors and unfoldings (or spatio-temporal diagrams, see below) related to them.
5. Describe regimes of sequential dynamics of the original neural network.

Note that in the case of identical thresholds the clusters of the same architecture produce the same responses. Thus, for networks with identical thresholds the number of the studied cases on step 2 (and complexity of CA rules) coincides with the number of different clusters, independently of the size of a network. For example, in a network with maximum M synaptic connections per neuron taking into account the synaptic dynamics (two different synaptical responses) the number of studied cases is equal to $M(M+3)/2$.

VI. EXAMPLE

We illustrate the approach on the example of a neural network modeled by the system of Eqs. (1)–(4) with an architecture presented on Fig. 5(a). In numerical simulations we use the values of parameters defined by Eqs. (14), (16) and the following values of threshold constants: $\theta_{13} = \theta_{23} = \theta_{32} = -0.03$, $\theta_{34} = 0.0$, $\theta_{41} = -0.02$. To conform to the architecture, all other thresholds in the system are set to 2.

It is easy to see that the network contains four elementary clusters: B_1-B_4, which are shown on Fig. 5(b). Figure 6 shows the graph of connections G corresponding to neural network on Fig. 5(a).

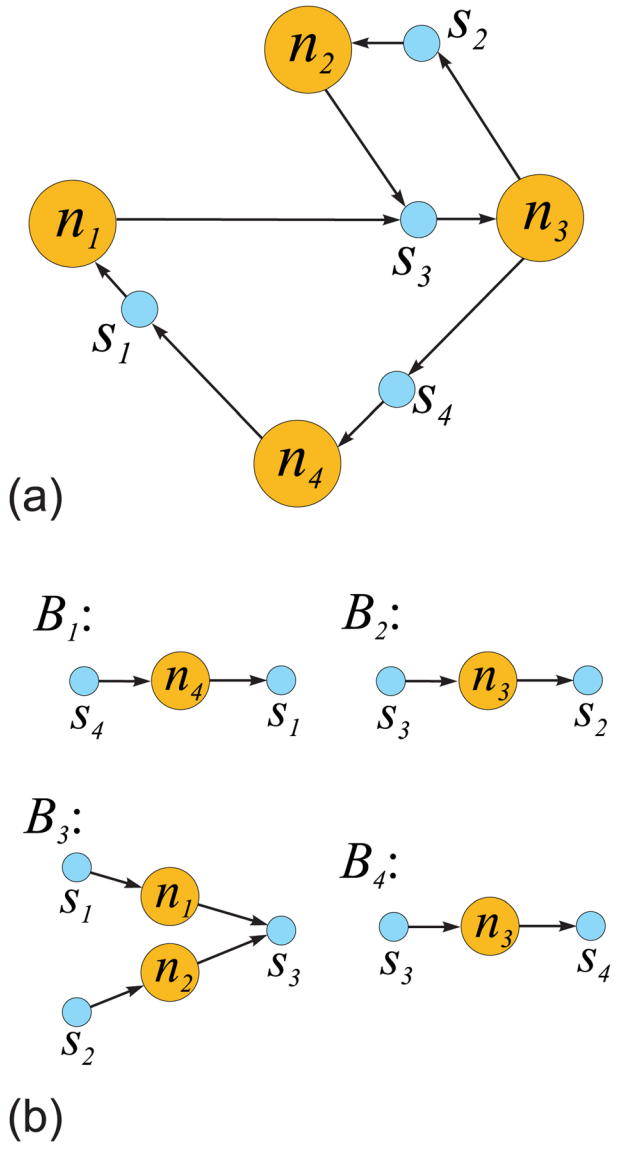

FIG. 5. (Color online) (a) The architecture of neural network and (b) elementary clusters of the network. Here n_i and s_i signify the neurons and synapses, respectively.

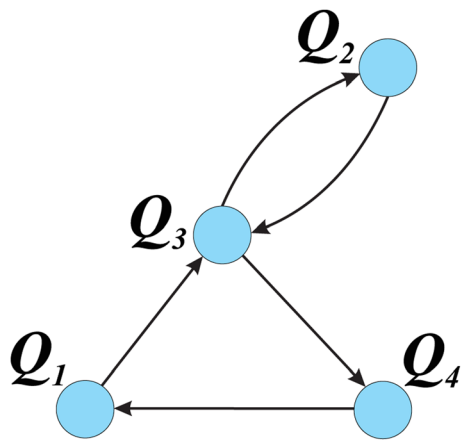

FIG. 6. (Color online) Graph of connections G corresponding to neural network presented in Fig. 5(a).

TABLE II. The rules $\overline{\psi_1} = F_1(\psi_1, \psi_4)$.

ψ_1	P_0	P_{11}	P_{21}	P_{22}
ψ_4				
P_0	P_0	P_0	P_{22}	P_0
P_{11}	P_{11}	P_0	P_{22}	P_0
P_{21}	P_0	P_0	P_{22}	P_0
P_{22}	P_{11}	P_0	P_{22}	P_0

Let us determine now the responses of each elementary cluster.

Cluster B_1: Numerical experiments show that the response of the synapse s_1 (while it is in the state P_0) to the action of the synapse s_4 is always of the minimal time scale T_1, independently of the state (P_{11} or P_{22}) of s_4. From here we obtain the rules of the CA presented in Table II.

Cluster B_2: The response of the synapse s_2 (if it is in the state P_0) is always of the minimal time scale T_1, independently of the state of s_3, so, the corresponding rules are shown in Table III.

Cluster B_3: The response of s_3, while it is in the P_0-state, is always of the minimal time scale T_1, independently of the state of s_1 and s_2, see Table IV for the corresponding rules of the CA.

Cluster B_4: The response of s_4, while it is in the P_0-state, is always of the double time scale, independently of the state of s_3, see Table V for the corresponding rules of the CA.

Thus, Tables II–V give us the full description of the rules F_i, $i = 1,...,4$, of our CA. Using these rules one may study the dynamics of the CA. We remind that we denote the states of synapses by numbers: $P_0 \to 0$, $P_{11} \to 1$, $P_{21} \to 2$, $P_{22} \to 3$. The CA has two attractors: A_0 and A_1. The attractor A_0 is the fixed point (0000). A fragment of the basin of A_0 is shown on Fig. 7(a). Such a form of the illustration is convenient and has been used before (see, for instance Refs. 13 and 16). We see that if all elements of the network is activated then all of them come to the rest state P_0. The attractor A_1 is the periodic trajectory (0010) → (0102) → (0013) → (1100) → (0010). A part of the basin of A_1 is shown on Fig. 7(b). The periodic points in the attractor are marked by the grey color.

According to the main property of cellular automata on finite graphs (see Appendix), every trajectory is eventually periodic and the attractors are periodic orbits. It is important to know the order in which elements become excited. For that, it is convenient to describe the motion on an attractor in the form of a spatio-temporal diagram or an unfolding, i.e., in the following way. We construct a figure in the plane with the horizontal axis corresponding to the time and with the vertical axis corresponding to the synapse number. Denote by C_{ki} the unit square on the plane with the lower-left corner having coordinates (k, i). Let us make C_{ki} black if $\psi_i(k) \neq 0$ and white if $\psi_i(k) = 0$. We note that the spatio-temporal diagrams (unfoldings) for a CA have been used before (see, for instance Refs. 13, 16, and 18).

The unfolding for A_0 is trivial—no elements are excited. The unfolding for A_1 is shown on Fig. 8. The unfoldings of CA describe, in fact, the regimes of sequential activation of synapses of a neural network. However, they allow to ascertain the regimes of sequential activation of neurons of the network as well. For instance, the narrow regions in the vicinity of transitions from black to white squares on Fig. 8 correspond to the phases of fast generation of spikes of corresponding neurons, while the other regions—to the non-oscillatory behavior of neurons. Thus, the unfoldings of CA allow to obtain whole information about the sequential dynamics of the network.

For the confirmation of the validity of these results, we have performed the direct numerical study of the original system (1)-(4) with architecture of Fig. 5(a). Results of numerics are presented on Fig. 9. The unfoldings of synaptic dynamics were constructed in the following way. We considered the rectangles $D_i(a, b)$, $i = 1, 2, 3, 4$ on the plane with the horizontal axis corresponding to the time and vertical axis corresponding to the synapse number. The height of $D_i(a, b)$ is 1, the width is $(b–a)$, the lower-left corner has

TABLE IV. The rules $\overline{\psi_3} = F_3(\psi_3, \psi_1, \psi_2)$.

ψ_3	P_0	P_{11}	P_{21}	P_{22}
ψ_1/ψ_2				
P_0/P_0	P_0	P_0	P_{22}	P_0
P_{11}/P_0	P_{11}	P_0	P_{22}	P_0
P_{21}/P_0	P_0	P_0	P_{22}	P_0
P_{22}/P_0	P_{11}	P_0	P_{22}	P_0
P_0/P_{11}	P_{11}	P_0	P_{22}	P_0
P_{11}/P_{11}	P_{11}	P_0	P_{22}	P_0
P_{21}/P_{11}	P_{11}	P_0	P_{22}	P_0
P_{22}/P_{11}	P_{11}	P_0	P_{22}	P_0
P_0/P_{21}	P_0	P_0	P_{22}	P_0
P_{11}/P_{21}	P_{11}	P_0	P_{22}	P_0
P_{21}/P_{21}	P_0	P_0	P_{22}	P_0
P_{22}/P_{21}	P_{11}	P_0	P_{22}	P_0
P_0/P_{22}	P_{11}	P_0	P_{22}	P_0
P_{11}/P_{22}	P_{11}	P_0	P_{22}	P_0
P_{21}/P_{22}	P_{11}	P_0	P_{22}	P_0
P_{22}/P_{22}	P_{11}	P_0	P_{22}	P_0

TABLE III. The rules $\overline{\psi_2} = F_2(\psi_2, \psi_3)$.

ψ_2	P_0	P_{11}	P_{21}	P_{22}
ψ_3				
P_0	P_0	P_0	P_{22}	P_0
P_{11}	P_{11}	P_0	P_{22}	P_0
P_{21}	P_0	P_0	P_{22}	P_0
P_{22}	P_{11}	P_0	P_{22}	P_0

TABLE V. The rules $\overline{\psi_4} = F_4(\psi_4, \psi_3)$.

ψ_4	P_0	P_{11}	P_{21}	P_{22}
ψ_3				
P_0	P_0	P_0	P_{22}	P_0
P_{11}	P_{21}	P_0	P_{22}	P_0
P_{21}	P_0	P_0	P_{22}	P_0
P_{22}	P_{21}	P_0	P_{22}	P_0

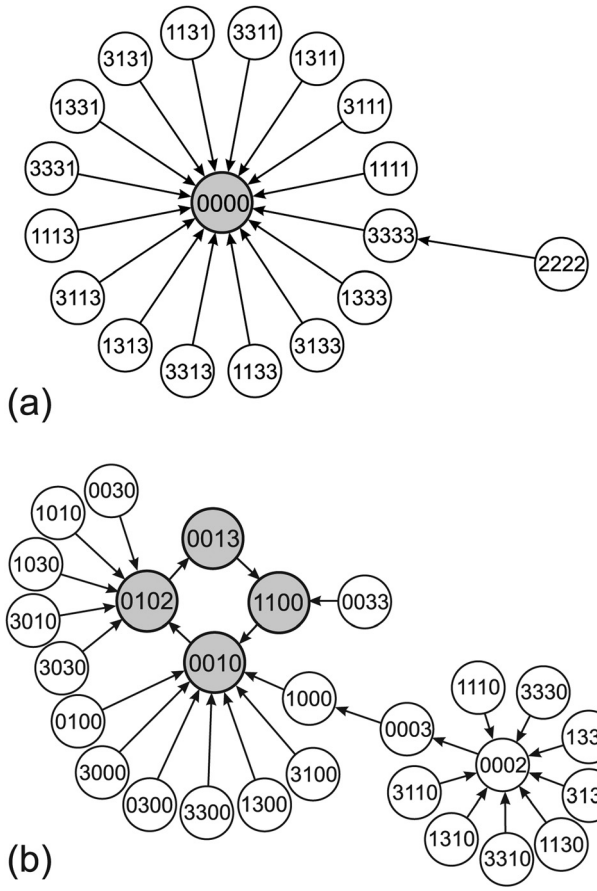

FIG. 7. (a) A part of the basin of the fixed point A_0 and (b) a part of the basin of the periodic attractor A_1.

coordinates (a, i), and it is black if the synapse i is active at the instant $t\left(s_i'(t) > 0\right)$, $a < t < b$ - see Fig. 9(a). Comparing the unfoldings of the CA and of the network, one may verify that the CA describes adequately the sequential dynamics of the network.

One can see that while the process of the activation of synapses (Figs. 9(a) and 9(b)) is in good correspondence with the unfolding for the CA (Fig. 8) it is not fully periodic. This is related to the fact that the resonance condition $T_2 = 2T_1$ is satisfied only with some (nonzero) accuracy. Nevertheless, first of all, the spacial order of activation of synapses is exactly the same as for the CA, and, secondly, temporal intervals of activation are approximately the same as for the CA up to the scaling factor T_1.

On Fig. 9(c) the change of membrane potentials for different neurons is presented. The temporal intervals of oscillatory activity and the rest of neurons occur in the order prescribed by the unfolding for synapses. The number of spikes might be different for different neurons and different times of observation, since it depends on the state of full network. Nevertheless, at an average the activation of the neuron network also occurs at the instants which are multiples of time scale T_1 (see Fig. 9(c)).

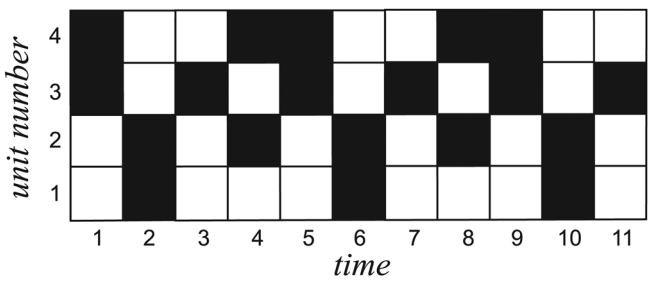

FIG. 8. Unfolding for the periodic attractor A_1 of CA.

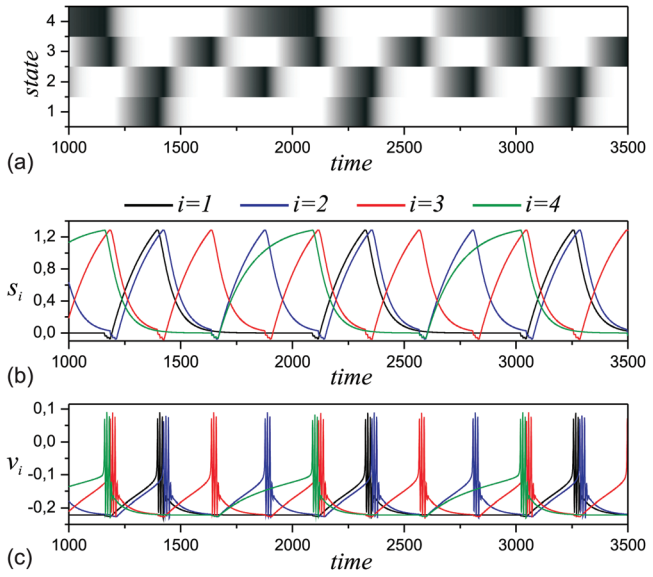

FIG. 9. (Color) Unfolding and realizations for established regimes in the network: (a) - unfolding; (b) - realizations for synapses; and (c) - realizations for neurons. The parameters are defined by Eqs. (14) and (16). The values of threshold constants are: $\theta_{13} = \theta_{23} = \theta_{32} = -0.03$, $\theta_{34} = 0.0$, $\theta_{41} = -0.02$. All other thresholds are set to 2.

VII. CONCLUSION

We have proposed an approach of the reduction of continuous sequential dynamics of excitatory neural networks to a discrete one, in the form of a CA on the graph of connections. In our approach the main role is played by the dynamics of synapses but not by the specific features of neurons. In fact, the approach requires to study only the responses of an individual synapse onto actions of neighboring (in graph of connections) synapses through corresponding neurons. As a result the numerical integration of the whole system of ODEs is not needed. Since the form of the neuron responses is not important, the approach is applicable to a broad set of networks including those consisting of neurons, which possess the neural excitability property (neurons of the class 2 excitability in the terminology of Izhikevich[2]).

It has been shown that under assumptions stated in $(E1)$-$(E7)$ one can construct a synaptic CA. Since a CA on a finite graph can have only attractors in the form of periodic trajectories, the corresponding sequential dynamics of the network in time is also periodic while in space it can be very complex. Remark that preliminary numerical results show that the CA-approach may work in a more general case. For example, when

$$\frac{T_2}{T_1} \simeq \frac{p}{q}$$

is the rational number with p and q being not large. Of course, in this case a CA will be more complex, but it will still have only finitely many attractors, each of which is just a periodic trajectory. Generally, the sequential dynamics of the network may be very complex. Nevertheless, it can be described in terms of rhythmic dynamics[37] on cellular automata. We suppose to study this problem elsewhere.

We have presented an example of application of the approach to the neural network with 4 neurons. It has been shown that the corresponding CA has the only nontrivial attractor. Generally, the number of attractors depends on the architecture of the graph of connections and the size of the network and can be large. Comparison of the results with direct numerical study of the original network has shown that the CA describes adequately the sequential dynamics of the network.

ACKNOWLEDGMENTS

V.S.A. acknowledges the financial support from Ministry of Education and Science Contract No. 02.740.11.5188. V.I.N. acknowledges the financial support from Ministry of Education and Science Contract Nos. 02.740.11.5188, 14.740.11.0348, P942 and RFBR Grant Nos. 09-02-00719, 09-02-91061. D.V.K. acknowledges the financial support from RFBR Grant No. 10-02-00643.

APPENDIX: CELLULAR AUTOMATON ON GRAPHS

The graph: Let us consider an oriented graph G consisting of N vertices which we identify with the numbers 1,2,...,N, and arrows joining some of them. We assume that every vertex is either a starting or an ending point of some arrow, or both. Given i denote by K_i the collection of vertices such that $j \in K_i$ if and only if there exists an arrow $j \to i$.

The function of state: To every i, we relate a collection of numbers $P_i = \{0,1,...,p_i - 1\}$. Sometimes it is said that the state i is in the value $\psi_i \in P_i$, or that the function of the state i gets the value ψ_i.

The phase space: The collection of the integer N-vectors $M = \{\psi = (\psi_1,\psi_2,...,\psi_N)\}$: $0 \le \psi_i \le p_i - 1$ will serve as the phase space of our dynamical system.

The rule: Given $i \in \{1, \ldots, N\}$, let us consider a function

$$f_i : \prod_{j \in K_i} P_j \to P_i,$$

i.e.,

$$f_i(\{\psi_j\}, j \in K_i) \in P_i.$$

The function f_i is called the rule of the cellular automaton at the site i.

The cellular automaton: Now, we define a dynamical system generated by the map $\mathfrak{F} : M \to M$ as follows

$$(\mathfrak{F}(\underline{\psi}))_i = f_i(\{\psi_j\}, j \in K_i) \tag{A1}$$

or $(\mathfrak{F}(\underline{\psi}))_i = \tilde{\psi}_i$ where

$$\tilde{\psi}_i = f_i(\{\psi_j\}, j \in K_i) \tag{A2}$$

This dynamical system is called the CA on graph G.

Attractors: The dynamics of the system (A1) is very simple, as follows from the following statement.

Lemma: Every point in M is ether $\mathfrak{F}$-periodic or eventually periodic.

Proof: Given an initial point $\underline{\psi}_0 \in M$, the point $\mathfrak{F}\underline{\psi}_0$ is either equal to $\underline{\psi}_0$ or not. If it is, the point $\underline{\psi}_0$ is a fixed point. If not, consider $\mathfrak{F}^2\underline{\psi}_0$. It is either one of $\underline{\psi}_0$, $\mathfrak{F}\underline{\psi}_0$ or not. If not, consider $\mathfrak{F}^3\underline{\psi}_0$, etc. The set M is finite, so there is m such that

$$\mathfrak{F}^m\underline{\psi}_0 \in \{\underline{\psi}_0, \mathfrak{F}\underline{\psi}_0, \ldots, \mathfrak{F}^{m-1}\underline{\psi}_0\}$$

i.e.,

$$\mathfrak{F}^m\underline{\psi}_0 = \mathfrak{F}^k\underline{\psi}_0, \quad k < m,$$

i.e.,

$$\mathfrak{F}^{m-k}(\mathfrak{F}^k\underline{\psi}_0) = \mathfrak{F}^k\underline{\psi}_0$$

and the point $\mathfrak{F}^k\underline{\psi}_0$ is $(m-k)$-periodic.

We say that a q-periodic trajectory $\Gamma = \{\underline{\psi}_1, \underline{\psi}_2, \ldots, \underline{\psi}_q\}$ is an attractor if there exists $\underline{\psi} \neq \Gamma$ such that $\mathfrak{F}^k\underline{\psi} \in \Gamma$ for some $k > 0$. A trivial corollary of the Lemma is that a CA on a graph has finitely many attractors.

[1]E. R. Kandel, J. H. Schwartz, and T. H. Jessell, *Principles of neural science* (Prentice-Hall International Inc., London, 1991).
[2]E. Izhikevich, *Dynamical systems in neuroscience* (MIT, Cambridge, MA, 2007).
[3]G. B. Ermentrout and D. H. Terman, *Foundations of Neuroscience* (Springer, New York/Dordrecht/Heidelberg/London, 2010).
[4]M. I. Rabinovich, P. Varona, A. I. Selverston, and H. D. I. Abarbanel, Rev. Mod. Phys. **78**, 1213 (2006).
[5]V. I. Nekorkin, Phys.-Usp. **51**, 295 (2008).
[6]M. Courbage and V. I. Nekorkin, Int. J. Bifurcation Chaos Appl. Sci. Eng. **20**, 1631 (2010).
[7]B. Ibarz, J. M. Casado, and M. A. F. Sanjuan, Phys. Rep. **501**, 1 (2011).
[8]O. Mazur and G. Laurent, Neuron **48**, 661 (2005).
[9]M. Stopfer, V. Jayaraman, and G. Laurent, Neuron **39**, 991 (2003).
[10]L. M. Jones, A. Fontanini, B. F. Sadacca, P. Miller, and D. B. Katz, Proc. Natl. Acad. Sci. U.S.A. **104**, 18772 (2007).
[11]V. S. Afraimovich, V. P. Zhigulin, and M. I. Rabinovich, Chaos **14**, 1123 (2004).
[12]M. I. Rabinovich and P. Varona, Front. Comput. Neurosci. **5**, 1 (2011).
[13]P. Ashwin, G. Orosz, J. Wordsworth, and S. Townley, SIAM J. Appl. Dyn. Syst. **6**, 728 (2007).
[14]M. A. Komarov, G. V. Osipov, J. A. K. Suykens, and M. I. Rabinovich, Chaos **19**, 015107 (2009).
[15]V. I. Nekorkin, D. V. Kasatkin, and A. S. Dmitrichev, Radiophysics Quantum Electron. **53**, 45 (2010).
[16]D. Terman, S. Ahn, X. Wang, and W. Just, Physica D **237**, 324 (2008).
[17]W. Just, S. Ahn, and D. Terman, Physica D **237**, 3186 (2008).
[18]S. Ahn, B. H. Smith, A. Borisyuk, and D. Terman, Physica D **239**, 515 (2010).
[19]C. Morris and H. Lecar, Biophys. J. **35**, 193 (1981).
[20]W. Rall, J. Neurophysiol. **30**, 1138 (1967).
[21]A. Destexhe, Z. F. Mainen: T. J. Sejnowski, in *Methods in Neuronal Modeling: From Ions to Networks* edited by C. Koch and I. Segev (MIT, Cambridge, MA, 1998).
[22]R. S. Zucker and W. G. Regehr, Annu. Rev. Physiol. **64**, 355 (2002).
[23]J. A. Varela, K. Sen, J. Gibson, J. Fost, L. F. Abbott, and S. B. Nelson, J. Neurosci. **17**, 7926 (1997).

[24]L. F. Abbott, J. A. Varela, K. Sen, and S. B. Nelson, Science **275**, 220 (1997).
[25]H. Markram, Y. Wang, and M. Tsodyks, Proc. Natl. Acad. Sci. U.S.A. **95**, 5323 (1998).
[26]M. Tsodyks, A. Uziel, and H. Markram, J. Neurosci. **20**, RC50 (2000).
[27]J. S. Dittman, A. C. Kreitzer, and W. G. Regehr, J. Neurosci. **20**, 1374 (2000).
[28]C.-C.J. Lee, M. Anton, C.-S. Poon, and G. J. McRae, J. Comput. Neurosci. **26**, 459 (2009).
[29]J. Trommershauser and A. Zippelius, Neurocomputing **38–40**, 65 (2001).
[30]J. Trommershauser, R. Schneggenburger, A. Zippelius, and E. Neher, Biophys. J. **84**, 1563 (2003).
[31]M. H. Hennig, M. Postlethwaite, I. D. Forsythe, and B. P. Graham, Neurocomputing **70**, 1626 (2007).
[32]H. Yang and M. A. Xu-Friedman, J. Neurophysiol. **99**, 2510 (2008).
[33]H. Shankaran, H.S. Wiley, and H. Resat, BMC Syst. Biol. **1**, 48 (2007).
[34]A. Y. C. Wong, B. P. Graham, B. Billups, and I. D. Forsythe, J. Neurosci. **23**, 4868 (2003).
[35]A. Morrison, M. Diesmann, and V. Gerstner, Biol. Cybern. **98**, 495 (2008).
[36]M. V. Hirsh, C. C. Pugh, and M. Shub, *Invariant manifolds (Lecture Notes in Mathematics)* (Springer-Verlag, Berlin, 1977).
[37]V. Afraimovich, E. Ugalde, J. Urias, *Fractal Dimensions and Poincare Recurrences* (Elsevier, Amsterdam, 2006).